Journal of Nuclear Materials 397 (2010) 55–60

Contents lists available at ScienceDirect

Journal of Nuclear Materials

journal homepage: www.elsevier.com/locate/jnucmat

Effect of hydrazine and formaldehyde on the corrosion of SS 304L in hot nitric acid environment

Geogy J. Abraham, V. Kain *, G.K. Dey

Materials Science Division, Bhabha Atomic Research Centre, Mumbai 400 085, India

ARTICLE INFO

Article history:
Received 10 June 2008
Accepted 4 December 2009

ABSTRACT

Electrochemical and immersion tests were carried out for SS 304L at 80 °C in 2 M nitric acid containing hydrazine and formaldehyde. The addition of hydrazine resulted in the higher anodic current and no appreciable change in weight loss. For formaldehyde, the reaction with nitric acid resulted in copious evolution of NO_2 gas and the subsequent dissolution of the gas in the solution. The open circuit potential (OCP) shifted to anodic direction by 300 mV. The OCP and polarization behaviour are controlled by the solution chemistry rather than the material surface.

1. Introduction

Stainless steels generally exhibit good corrosion resistance in nitric acid owing to the fact that they are passivated forming a thin oxide film based on Cr_2O_3. Type 304L stainless steel (SS) is the preferred construction material for chemical plants and spent fuel reprocessing and waste management plants where nitric acid is used extensively. In fuel reprocessing plants, nitric acid is used from room temperature to boiling point; in dilute to concentrated solution; and also in the presence of several fission products and oxidizing ions [1].

The nitric acid solutions of concentrations up to 6 M and temperatures up to 120 °C are encountered in the Purex process followed by the reprocessing plant. SS 304L is the most commonly used material. However, there are also other materials that are in use such as SS 304L Nitric Acid Grade (NAG) stainless steel, SS 310L, SS 310Cb, Titanium, Zirconium and Ti–5% Ta, It is evident that only a few materials can be used for applications involving severe nitric acid environment [2]. It is well known that SS 304L undergoes several localized type of corrosion namely, end-grain attack, transpassive dissolution, vapour phase attack etc., in addition to the predominant intergranular corrosion (IGC). The working potential range of SS 304L components in a reprocessing plant are close to the transpassive potential [3].

In the Purex processing of irradiated fuel, dissolution of uranium metal or uranium dioxide involves oxidation to the hexavalent uranyl ion accompanied by the copious generation of NO_x gases The produced NO_x gases dissolve in aqueous solution to produce nitrous acid (HNO_2). Hydrazine treatment of the Purex feeds is to reduce tetravalent Pu in order to prevent its extraction into organic phase (TBP) along with uranium. It has been recommended for improving the decontamination for ruthenium [4]. In the uranium extraction column, hydrazine is used as a scrub to enhance the ultimate purity of the uranium product [4]. Hydrazine as a stabilizer removes traces of nitrous acid which initiate the oxidation of divalent iron and trivalent plutonium in nitric acid systems. The reaction of hydrazine with nitrous acid gives HN_3, N_2O and N_2 as shown in Eqs. (1) and (2) [4].

$$N_2H_5^+ + HNO_2 \rightarrow HN_3 + 2H_2O + H^+ \quad (1)$$

$$HN_3 + HNO_2 \rightarrow N_2O + N_2 + H_2O \quad (2)$$

Formaldehyde is used for decomposing excess nitric acid in Purex process solution. The decomposition of nitric acid at different concentrations of the acid is shown in Eqs. (3)–(5). At lower concentrations of nitric acid (<0.5 N), the final products of decomposition are CO_2, NO and NO_2 [5–8].

$$4HNO_3 + CH_2O \rightarrow 4NO_2 + CO_2 + 3H_2O \ (16\text{—}8\ N) \quad (3)$$

$$4HNO_3 + 3CH_2O \rightarrow 4NO + 3CO_2 + 5H_2O \ (8\text{—}2\ N) \quad (4)$$

$$2HNO_3 + CH_2O \rightarrow HCOOH + 2NO_2 + H_2O \ (2\ N) \quad (5)$$

The objective of this study was to examine the effect of addition of hydrazine and formaldehyde in nitric acid medium on the dissolver tank made of SS 304L. Open circuit potential measurement, potentiodynamic and potentiostatic studies at a temperature of 80 °C were carried out for SS 304L in 2 M HNO_3 with different concentration of hydrazine and formaldehyde. Also weight loss experiments were carried out for the samples at 80 °C in the same environment.

---

* Corresponding author. Tel.: +91 22 25595067; fax: +91 22 25505151.
E-mail address: vivkain@barc.gov.in (V. Kain).

0022-3115/$ - see front matter © 2009 Elsevier B.V. All rights reserved.
doi:10.1016/j.jnucmat.2009.12.006

2. Experimental procedure

2.1. Materials

Type 304L stainless steel samples having a composition in wt.% of 0.025 C, 18 Cr, 9.3 Ni, 1 Mn, 0.017 S, 0.026 P and Balance Fe was used. The specimens were in the form of coupons having dimension of 30 mm × 10 mm × 1 mm with stainless wire leads spot welded to the coupon for electrical connection. The exposed area of the working electrode was 250 mm°. The specimens were polished to diamond finish and cleaned with acetone. Type 304L stainless steel samples were annealed at 1050 °C for ½ h and water quenched.

2.2. Environments

Nitric acid solution of 2 M concentration was prepared from analytical reagent (AR) grade nitric acid using double distilled water. Hydrazine was added in the form of hydrazine nitrate having a 10 M concentration. Formaldehyde added was AR grade of 40% w/v solution. Hydrazine nitrate ($N_2H_5{\cdot}NO_3$) and formaldehyde (HCHO) were added to 2 M HNO_3 solution in the ratio 2.5 mL and 5.0 mL of hydrazine nitrate: 600 mL of 2 M HNO_3 and 2.5 mL and 5.0 mL of HCHO: 600 mL of 2 M HNO_3. Total solution in each electrochemical experiment was 602.5 mL or 605 mL. These correspond to 0.042 mol/L and 0.083 mol/L of hydrazine and 0.055 mol/L and 0.111 mol/L of formaldehyde. The experiments were carried out at 80 °C.

2.3. Electrochemical testing

The electrochemical set up consisted of a standard three electrode electrochemical cell with platinum as the counter electrode and saturated calomel electrode (SCE) as the reference electrode. The SCE was at room temperature and was connected to the cell via a luggin probe. The cell also had a temperature controlling device and a condenser to maintain the concentration of the solution. Electrochemical measurements were performed with Solartron 1287 potentiostat. In this paper V_{SCE} refers to the potential in volts when measured against saturated calomel electrode.

3. Results

3.1. OCP measurements

The OCP measurements were carried out for SS 304L in 2 M HNO_3 solution, 2 M HNO_3 containing hydrazine and 2 M HNO_3 containing formaldehyde solution at 80 °C and results are presented in Figs. 1 and 2. The OCP of SS 304L increased with time in nitric acid. After the potential reached the steady value, 5 mL formaldehyde was added to 2 M nitric acid (600 mL) which increased the OCP further (+0.72 V_{SCE}). The second case in which another 2.5 mL (i.e. a total of 5 mL) of formaldehyde was added to 2 M HNO_3 (600 mL), it increased the potential further but to a smaller extent (+0.78 V_{SCE}). In the same figure (Fig. 1), variation of potential is shown, when the formaldehyde (5 mL) was mixed with nitric acid before immersion of the sample. In this case, the increase was sharp but the final potential was roughly the same as in the previous case. Thus, the final potential was not affected by prefilming of the alloy surface in nitric acid. The OCP measured in 2 M HNO_3 solution containing hydrazine was quite different from this (Fig. 2). In this case, there was initial increase in potential followed by a decrease and a plateau at about 0.5 V_{SCE} and final settlement of potential at the value as found in nitric acid without any addition (Fig. 1). The initial increase in the potential is the result of adsorption of hydrazine on the sample surface while the drop in value of OCP is due to the oxidation of hydrazine by nitric acid to nitrogen. This is supported by the Latimer diagram in acid solutions [9] which shows that the redox potentials shift in cathodic direction when $N_2H_5^+$ is reduced to N_2.

3.2. Polarization studies

The potentiodynamic polarization experiments were carried out in the potential range of -0.2 V_{OCP} to +1.6 V_{SCE}. The scan rate used was 0.5 mV/s and the polarization run was stopped after attaining the transpassive dissolution. Polarization runs were taken after stabilization of potential (approximately 1 h). Fig. 3 represents the polarization curve of SS 304L in 2 M HNO_3 at 80 °C and in 2 M HNO_3 containing hydrazine (600 mL of 2 M HNO_3 + 5 mL of hydrazine nitrate of 10 M concentration). As shown in Fig. 3, SS 304L showed a polarization curve in nitric acid with low anodic current and no active/passive transition. The currents were higher in presence of hydrazine (Fig. 3b). The polarization in presence of 2.5 mL hydrazine was similar to that with 5 mL hydrazine and was not included for clarity in Fig. 3. The corrosion potential (E_{corr}) is low (more cathodic) in presence of hydrazine as compared to that in pure nitric acid. The polarization behaviour of SS 304L in nitric acid in presence of formaldehyde is shown in Fig. 4. The corrosion potential (E_{corr}) shifted systematically in the anodic direction with increase in formaldehyde concentration (Fig. 4a–c). As can be seen from the Fig. 4, the transpassive potentials are lowered (in the cathodic direction) in presence of formaldehyde. The plateau current was not seen in the presence of formaldehyde. The

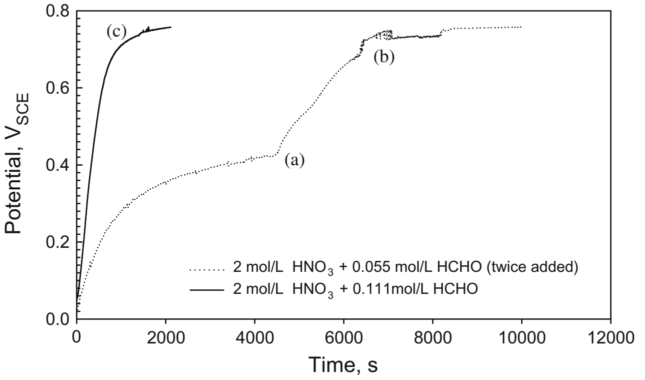

Fig. 1. Open circuit potential of SS 304L in 2 M HNO_3 (2 mol/L) with addition of formaldehyde at 80 °C: (a) addition of 0.055 mol/L; (b) addition of another 0.055 mol/L HCHO; and (c) 0.111 mol/L of HCHO in nitric acid.

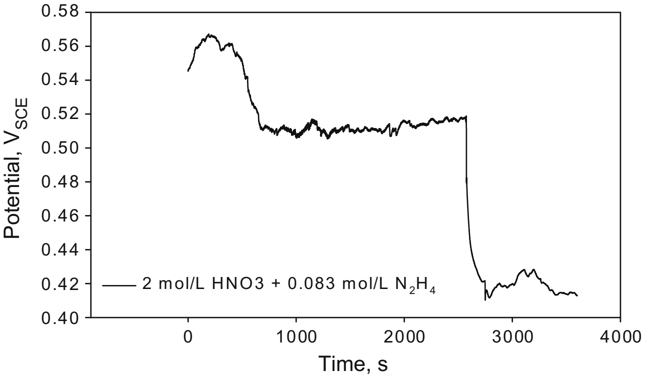

Fig. 2. Open circuit potential of SS 304L in 2 mol/L HNO_3 including 0.083 mol/L hydrazine.

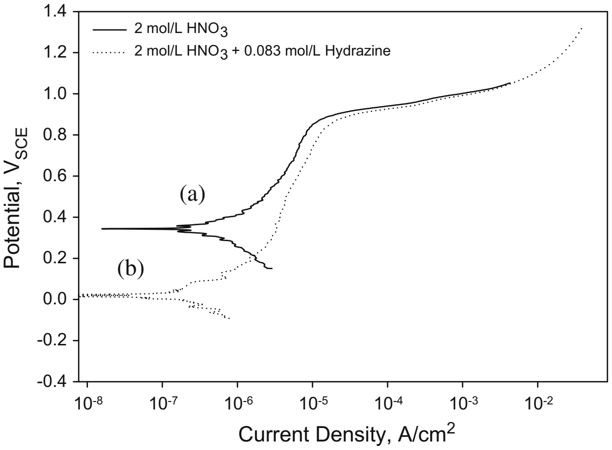

Fig. 3. Polarization curve of SS 304L in 2 mol/L HNO_3 including hydrazine at 80 °C: (a) 2 mol/L HNO_3 and (b) 0.083 mol/L N_2H_4, scan rate 0.5 mV/s.

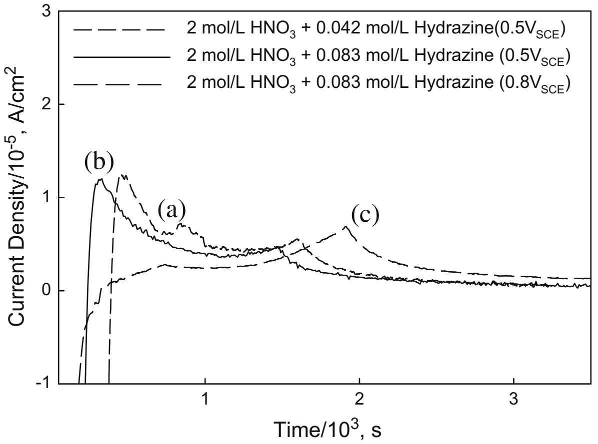

Fig. 5. Current–time plot of SS 304L in 2 mol/L HNO_3 and hydrazine at 0.5 V_{SCE} and 80 °C: (a) 0.042 mol/L; (b) 0.083 mol/L; and (c) 0.083 mol/L at 0.8 V_{SCE}.

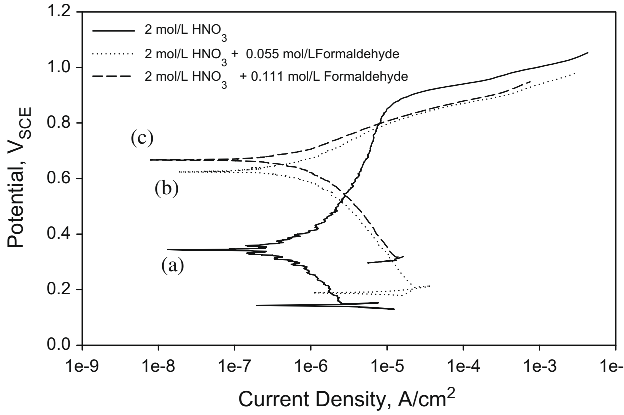

Fig. 4. Polarization curve for SS 304L in 2 mol/L HNO_3 including formaldehyde at 80 °C: (a) 2 mol/L HNO_3; (b) nitric acid with 0.055 mol/L HCHO; and (c) nitric acid with 0.111 mol/L HCHO, scan rate 0.5 mV/s .

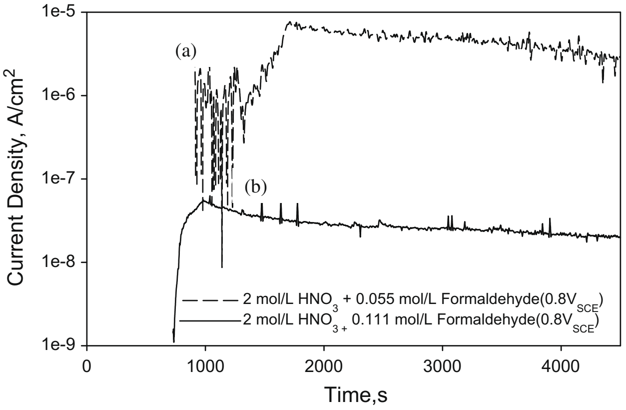

Fig. 6. Current–time plot of SS 304L in 2 mol/L HNO_3 including HCHO at 0.8 V_{SCE} and 80 °C: (a) 0.055 mol/L HCHO and (b) 0.111 mol/L HCHO.

current was higher in presence of 2.5 mL formaldehyde than in the presence of 5 mL formaldehyde at corresponding potentials.

3.3. Potentiostatic studies

In this study, the potentiostatic experiments are done at 80 °C. The potentiostatic experiments were carried out at 0.5 V_{SCE} and 0.8 V_{SCE}. These potentials were selected as these were well inside the passive potential region of SS 304L in nitric acid and less than the transpassive potential. For these experiments, samples were scanned after attaining a steady OCP (about an hour after immersion), from -0.2 V_{SCE} (vs. OCP) to the specific potential and then held there for up to 10,000 s. The samples were weighed before and after the tests for weight loss. The resulting current time plots are given in Figs. 5 and 6. Fig. 5 shows the *i*–*t* curve for SS 304L in nitric acid and nitric acid containing hydrazine at 0.8 V_{SCE}. The current was positive (anodic) in all the cases at this potential. The anodic current, charge consumed and weight loss were low when the potentiostatic study was done in nitric acid. There was increase in current and charge on addition of hydrazine but weight loss was not affected much. Fig. 6 shows the *i*–*t* plot obtained at 0.8 V_{SCE} in solution containing nitric acid and formaldehyde. The charge consumed as well as the weight loss was high in presence of 2.5 mL HCHO than in the presence of 5 mL HCHO. During the scanning to attain the desired potential, the current measurements observed were as high as 40 mA/cm^2 in first part of the scan with a corresponding charge of 4 C/cm^2. After about 1000 s, the current was of the order of 10 mA, still one fold higher than in presence of 5 mL HCHO. This was in accordance with the polarization behaviour mentioned above. When the experiment was carried out at 0.5 V_{SCE}, the *i*–*t* curves show negative (cathodic) current, as in Fig. 7. Magnitude of charge consumed as well the weight loss increased with increase in the concentration of HCHO as shown in Table 1. Fig. 8 shows micrograph of the sample after the potentiostatic experiments in 0.8 V_{SCE} presence of 2.5 mL formaldehyde in 2 M nitric acid at 80 °C. The grain boundary etching is very clear in the microstructure which goes to show that the stainless steel surface is in a potential region that is close to the transpassive region.

3.4. Immersion tests

Immersion tests were performed on SS 304L in 2 M HNO_3 containing formaldehyde and hydrazine separately. The duration of the experiments was 2 weeks. Results of these tests are included in Table 1. In all, the corrosion rate was less and was not affected significantly by addition of hydrazine. However, there was some increase in the weight loss in presence of formaldehyde.

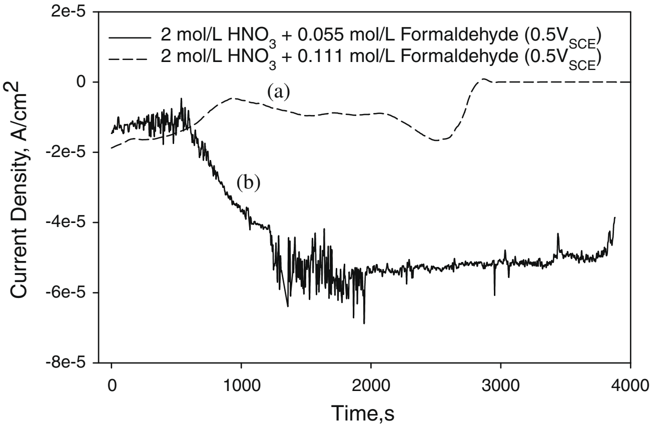

Fig. 7. Current–time plot of SS 304L in 2 mol/L HNO_3 including HCHO at 0.5 V_{SCE} and 80 °C: (a) 0.055 mol/L HCHO and (b) 0.111 mol/L HCHO.

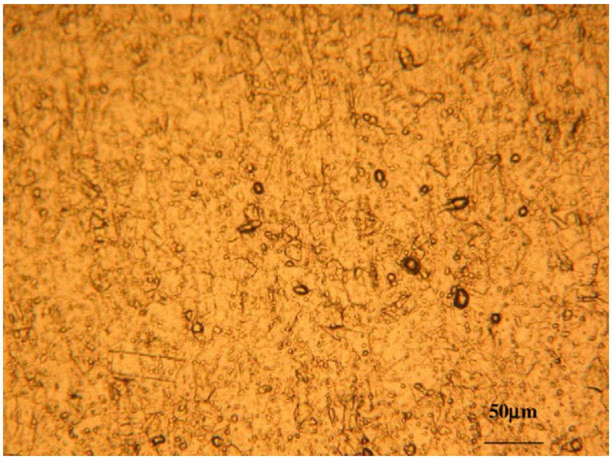

Fig. 8. Micrograph of SS 304L etched in 2 mol/L HNO_3 + 0.055 mol/L HCHO (0.8 V_{SCE}) at 80 °C for 6000 s.

4. Discussion

4.1. Corrosion in nitric acid: mechanism

According to Razygraev et al. [10], the global reaction of reduction of nitric acid is

$$HNO_3 + H^+ + e^- \rightarrow NO_2 + H_2O \tag{6}$$

and it is followed by a heterogeneous mechanism (at anodic potentials/acid concentration above 8 M).

$$NO_2 + e^- \rightarrow NO_2^- \tag{6i}$$

$$NO_2^- + H^+ \rightarrow HNO_2 \tag{6ii}$$

$$HNO_2 + HNO_3 \rightarrow 2NO_2 + H_2O \tag{6iii}$$

In parallel, the following reactions (as per the homogeneous mechanism, at lower potentials/concentrations of acid) also occur

$$HNO_2 + H^+ \rightarrow NO^+ + H_2O \tag{6iv}$$

$$NO^+ + e^- \rightarrow NO \tag{6v}$$

$$NO + HNO_3 \rightarrow HNO_2 + NO_2 \tag{6vi}$$

The electro active species in reduction of nitric acid is nitrous acid. The nitric acid reduction is an autocatalytic mechanism which constitutes a charge transfer step and a chemical reaction which regenerates the electroactive species as shown by the above reactions. This result in the formation of an extra half mole of nitrous acid for each mole of nitrous acid destroyed. The self passivation of the stainless steel is attributed to the autocatalytic reduction of nitric acid (Eqs. (6) and (6i)–(6vi)) [16]. The heterogeneous mechanism, has been shown to occur at more anodic potentials (>0.5 V_{SCE}) and both the mechanisms occur simultaneously at lower potentials. The present system consists of HNO_3, HNO_2, NO, NO_2. Reduction of nitric acid in presence of NO and NO_2 may be [13]

$$NO_2 + H_2O \rightarrow NO_3^- + 2H^+ + e \tag{7}$$

$$NO + 2H_2O \rightarrow NO_3^- + 4H^+ + 3e \tag{8}$$

In presence of these species, the potential of ~0.8 V_{SCE} is the thermodynamic potential of reaction (7) and (8). Hence, nitric acid containing NO, NO_2 actually increases the potential of stainless steel to positive (anodic) potential. Potential of 1 V_{SCE} has been reported [13] in15.8 M HNO_3 at 100 °C. The redox potentials of the solution are dependant on the HNO_2/HNO_3 ratio. In the lower concentration regime of nitric acid (<8 mol/l) the HNO_2 regeneration is controlled by the presence of NO while at higher concentrations NO_2 play a role in regeneration of the electroactive species. This makes the medium excessively oxidizing and passive film dissolution takes place as the stainless steel potentials are shifted to the transpassive region where oxidation of Cr(III) to Cr(VI) takes place. The N_2 and N_2O are other possible products but are electrochemically inert in the potential range 0.5–1.5 V_{SCE}. HNO_2 is also formed by reduction of NO_2 and NO from the reaction.

$$NO_2 + NO + H_2O \rightarrow 2HNO_2 \tag{9}$$

In presence of nitric acid alone the corrosion potential for SS 304L was about 0.5 V_{SCE} showing a continuous passivation trend. The corrosion potentials attained are low due to the lower concentration of nitric acid taken which results in the slower rate of regeneration of HNO_2. The NO_2 formed in this case is unstable and hence is drawn back towards HNO_2 formation. In these polarization experiments there was no clear active–passive transition

Table 1
Weight loss in immersion tests and charge consumed in potentiostatic etching experiments in nitric acid + formaldehyde and nitric acid + hydrazine environment.

Environment	Immersion test (2 weeks at 80 °C) (mpy)/(mm/y)	Potentiostatic studies at 80 °C for 10,000 s			
		Charge consumed[a] (C/cm^2)		Weight loss (mpy)/(mm/y)	
		0.5 V_{SCE}	0.8 V_{SCE}	0.5 V_{SCE}	0.8 V_{SCE}
(a) 2 M HNO_3 (600 mL)	12.5/0.32	0.003	0.004	49.7/1.26	51/1.295
(a) +2.5 mL HCHO	208/5.28	−0.03	4.0*/0.1	218/5.54	250/6.35
(a) +5 mL HCHO	217/5.12	−0.164	0.028	639/16.2	103/2.62
(a) +2.5 mL N_2H_4	14.0/0.35	0.007	0.012	47/1.194	52/1.32
(a) +5 mL N_2H_4	13.5/0.34	.015	0.03	55/1.397	53.35/1.35

[a] Charge normalized for 5000 s.
* Including high current value.

seen at potentials slightly anodic to OCP. However, a transpassive potential of 0.9 V_{SCE} is clearly observed in 2 M nitric acid at 80 °C. In the potentiostatic studies the weight loss and the anodic currents were low for the samples exposed in nitric acid as the regeneration rates for HNO_2 were slow for the present concentration as the by product is NO since NO_2 is thermodynamically unstable.

4.2. Corrosion in presence of hydrazine: mechanism

The reaction of hydrazine with nitrous acid gives HN_3, N_2O and N_2 as seen in Eqs. (1) and (2). The OCP value did not change much for hydrazine addition to nitric acid due to the reaction products which do not have much effect on the potentials and the addition of hydrazine results in scavenging of HNO_2 (Eqs. (1) and (2)) and reduces the reduction reaction of nitric acid. The formation of NO and NO_2 will be less as the HNO_2 concentration in the solution is reduced. In the polarization studies the corrosion potential shifted to the cathodic side in presence of hydrazine (Fig. 3). Hence, the oxidation of hydrazine results in HNO_2 scavenging which changes the HNO_2/HNO_3 ratio and thereby reduces the corrosion potential.

In presence of hydrazine, the current was more as compared to that in nitric acid (in the potential range of 0.5–0.9 V_{SCE} as seen from Fig. 3) but weight loss was not affected significantly. The increase in the current can be attributed to the oxidation of hydrazine in the solution. In presence of higher concentration of hydrazine, secondary passivity behaviour was found wherein there is a distinctive region near to the 1 V_{SCE} that shows a pseudo passive behaviour probably because of the adsorption of the reduction products of Cr(VI) ions by hydrazine on the surface of the specimen in the transpassive region [11]. The hydrazine reduction takes place by a two electron transfer to N_2 while the chromium(VI) frequently behaves as a two electron oxidant with an initial formation of a Cr(VI)–hydrazine complex. The reaction of hydrazine with Cr(VI) can be represented by Eq. (10) [13]

$$4CrO_4H^- + 3N_2H_5^+ + 13H^+ + 8H_2O \rightarrow 4[Cr(OH_2)_6]^{+3} + 3N_2 \qquad (10)$$

As seen from Fig. 5, *i–t* curve indicates different mechanism working in plain nitric acid solution and in presence of hydrazine. According to Cames [12], hydrazine gets oxidized to nitrogen by a four electron transfer or to nitrogen and ammonium ion with one electron transfer. At 0.65 V_{SCE}, hydrazine can be selectively oxidized to nitrogen by four electron transfer. Hydrazine oxidation proceeds with electrochemical yield of 100%. The current values though higher in case of the potentiostatic experiments the weight loss is less due to scavenging of nitrous acid by hydrazine which eventually stops the autocatalytic reduction reaction in the solution.

4.3. Corrosion in presence of formaldehyde: mechanism

Formaldehyde reduction action is much stronger than hydrazine. It reduces nitric acid to HNO_2, NO and NO_2. There is a finite incubation period for this reaction. Dark brown fumes were observed over the solution and got cleared after some time. The reduction products of nitric acid, such as nitrous oxide, nitrogen dioxide and HNO_2 lead to an increase in reduction rate. With the increase in reduction rate, the current density in reduction increases and cathodic part of the current–potential curve shifts in the anodic direction. Hence there is a shift in the corrosion potential. Both NO and NO_2 favor an anodic shift in the corrosion potential. The potential of SS 304L found in nitric acid in presence of HCHO in the present study was in the same range of 0.8 V_{SCE} as reported earlier [14].

Armstrong and Cleland [15], Takeuchi and Whillock [16] observed a decrease in solution redox potentials of nitric acid on bubbling NO through solution while the E_{corr} of stainless steel increased when NO_2 or NO was bubbled through the nitric acid; more so in case of NO_2. The NO_2 purging acts as an oxidizing agent for SS and also the anodic current increases in presence of NO_2. However, there was no enhancement of corrosion rate but it could be attributed to the oxidation of nitrate to nitrite ions in the solution. In the present case, both NO and NO_2 may be generated on addition of formaldehyde. No attempt was made to detect NO but presence of NO_2 was clear by its deep brown colour. In nitric acid solution containing formaldehyde, the shift in potential was very large. Potential rise particularly in presence of formaldehyde and the polarization curves can be explained in terms of autocatalytic/catalyzed reduction of nitric acid by NO and NO_2 [15–18]. The OCP of steel has been reported to increase with temperature and concentration of nitric acid. Cr(VI) and Cr(III) ions also play a role in determining OCP as Cr(VI) ions are powerful oxidants their presence in the solution containing NO_x will be beneficial in reducing the corrosion potential thus reducing the transpassive corrosion rate. In the present study the effect of these ions could not be seen as duration of electrochemical experiments were short. The system SS 304L in nitric acid containing formaldehyde or hydrazine behaves as an unstable system in the early period of immersion. Polarization curves taken immediately after immersion were very noisy and reproducibility was poor. On stabilizing, it was much more stable and reproducible.

It appears that the complete polarization in experiments reported for this study consists of two separate polarizations; one at the lower potential (primary OCP at cathodic potentials) and another at the observed or stable OCP (secondary OCP). The mixed potentials obtained from different slopes determine the observed OCP. The exact nature of the secondary OCP is not clear. It is taken that the secondary OCP results from a mixed potential of anodic passive dissolution and cathodic reduction of NO_3^- and/or NO_2.

However, as explained by Kolman et al. [17], the heterogeneous mechanism occurs at more anodic potentials while the homogenous mechanism, in parallel with the heterogeneous mechanism, occur at lower potentials. The cathodic reaction is probably the reduction of nitrogen oxides. Thus, it appears that the secondary OCP arises from the mixed potential comprising of anodic dissolution and cathodic reduction of nitrogen compounds. In potentiostatic experiments at 0.8 V_{SCE}, the current was positive (anodic) while at 0.5 V_{SCE}, the current was negative (cathodic) and its magnitude varied with concentration of formaldehyde. This potential was slightly negative (cathodic) to OCP in presence of 2.5 mL formaldehyde, but more negative (cathodic) to OCP in presence of 5 mL of formaldehyde. Hence the negative (cathodic) charge was high at this potential. There should be no weight loss at a negative (or cathodic) potential. But corresponding weight loss indicates loss of metal due to forced cathodic reaction mentioned above. Particularly high current in case of 2.5 mL formaldehyde, is due to scanning the sample from a potential -0.2 V_{OCP}. Only in this case, some grain boundary etching was observed as shown in Fig. 8. The grain boundary etching indicates that the potentials have reached the transpassive domain of the steel due to the reduction of nitric acid by formaldehyde and formation of NO_2. As earlier stated, this shifts the potential to the transpassive regime resulting in the forced metal dissolution. The corrosion rate is less but if slightly reducing atmosphere is generated, the metal loss will increase.

5. Conclusions

The effect of the addition of hydrazine and formaldehyde in nitric acid has been studied. Polarization and weight loss experimental data have been reported. The corrosion rate of SS 304L was low in 2 M HNO_3 and not effected significantly by addition of hydrazine. The addition of formaldehyde in nitric acid makes the environment more aggressive for SS 304L. The OCP of stainless steel becomes more positive (anodic) in presence of formaldehyde. The electrochemical behaviour as well as weight loss of stainless steel is controlled by solution chemistry rather than change in the surface state. This has been explained on the basis of autocatalytic reduction of nitric acid.

References

[1] U. Kamachi Mudali, R.K. Dayal, J.B. Gnanmoorthy, J. Nucl Mater. 203 (1993) 73–82.

[2] Baldev Raj, U. Kamachi Mudali, T. Jayakumar, K.V. Kasiviswanathan, R. Natarajan, Sadhana 25 (Part 6) (2000) 519–559.

[3] Baldev Raj, U. Kamachi Mudali, Materials challenges at the back end of the fuel cycle, in: INSAC – 2001, CAT, Indore, 2001, p. 142.

[4] S.V. Kumar, M.N. Nadakarni, A. Ramanujam, M. Venkatesan, V. Gopalakrishnan, J.A. Kazi, BARC Report No. 782, 1974.

[5] S.V. Kumar, M.N. Nadkarni, P.C. Mayankutty, N.S. Pillai, S.S. Shinde, BARC Report No. 781, 1974.

[6] T.V. Healy, J. Appl. Chem. 8 (1958) 553.

[7] T.F. Evans, “The pilot plant denitration of Purex wastes with formaldehyde,” HW 58587, 1959.

[8] R.C. Forsman, G.C. Obera, “Formaldehyde treatment of Purex radioactive wastes,” HW 79622, 1963.

[9] Allen J. Bard (Ed.), Encyclopedia of Electrochemistry of the Elements, vol. VIII, Marcel Dekker, Inc.,, New York, 1976, p. 326.

[10] V.P. Razygraev, M.V. Lebedeva, S.A. Kabakchi, E.Y. Ponomareva, R.S. Balovneva, L.P. Lobanova, J. App. Chem. USSR 61 (1988).

[11] Geogy J. Abraham, 2004, unpublished work.

[12] B. Cames, Investigation of the Direct and Indirect Electrochemical Oxidation of Hydrazine in Nitric Acid Medium on Platinum, Report No. CEAR 5779, 1997, 199.

[13] M.T. Beck, D.A. Durham, J. Inorg. Nucl. Chem. 32 (1970) 1971–1977.

[14] V.M. Sadagopa, V.M.S. Ramanayam, S. Sundaram, N. Venkatasubramanian, Inorg. Chim. Acta. 13 (1975) 33–139.

[15] R.D. Armstrong, G.E. Cleland, J. Appl. Electrochem. 28 (1998) 1205.

[16] M. Takeuchi, G.O. Whillock, Brit. Corros. J. 37 (2002) 99.

[17] D.G. Kolman, D.K. Ford, D.P. Butt, T.O. Nelson, Corros. Sci. 39 (1997) 2162.

[18] F. Balbaud, G. Sanchez, P. Fauvet, G. Satarini, G. Picard, Corros. Sci. 42 (2000) 1685.